Turing space in reaction-diffusion systems with density-dependent cross diffusion

E. P. Zemskov,[1,*] K. Kassner,[2,†] M. J. B. Hauser,[3,‡] and W. Horsthemke[4,§]

[1]*Department of Continuum Mechanics, Computing Centre of the Russian Academy of Sciences, Vavilova 40, 119333 Moscow, Russia*

[2]*Institut für Theoretische Physik, Otto-von-Guericke-Universität, Universitätsplatz 2, 39106 Magdeburg, Germany*

[3]*Institut für Experimentelle Physik, Otto-von-Guericke-Universität, Universitätsplatz 2, 39106 Magdeburg, Germany*

[4]*Department of Chemistry, Southern Methodist University, Dallas, Texas 75275-0314, USA*

(Received 9 November 2012; published 13 March 2013)

Reaction-diffusion systems with cross-diffusion terms that depend linearly on density are studied via linear stability analysis and weakly nonlinear analysis. We obtain and analyze the conditions for the Turing instability and derive a universal form of these conditions. We discuss the features of the pattern-forming regions in parameter space for a cross activator-inhibitor system, the Brusselator model, and for a pure activator-inhibitor system, the two-variable Oregonator model. The supercritical or subcritical character of the Turing bifurcation for the Brusselator is determined by deriving an amplitude equation for patterns near the instability threshold.

DOI: 10.1103/PhysRevE.87.032906 PACS number(s): 82.40.Bj, 82.40.Ck, 05.45.−a, 47.54.−r

I. INTRODUCTION

Reaction-diffusion systems with cross-diffusion terms that depend linearly on the density, described by equations [1]

$$\frac{\partial u}{\partial t} = F_1(u,v) + D_{11}\frac{\partial^2 u}{\partial r^2} + D_{12}\frac{\partial}{\partial r}\left(u\frac{\partial v}{\partial r}\right), \quad (1.1a)$$

$$\frac{\partial v}{\partial t} = F_2(u,v) + D_{21}\frac{\partial}{\partial r}\left(v\frac{\partial u}{\partial r}\right) + D_{22}\frac{\partial^2 v}{\partial r^2}, \quad (1.1b)$$

for two components $u = u(r,t), v = v(r,t)$ and constant diffusion coefficients $D_{ij}, i,j = 1,2$, implement the Keller-Segel ansatz [2,3] for the chemotactic response of microscopic organisms to macroscopic chemical gradients. In such a description the (diagonal or main) diffusion coefficients, D_{ii}, are always positive, whereas the chemotactic (cross-diffusion) coefficients, $D_{ij}, i \neq j$, may be positive or negative [2]. Thermodynamics imposes the additional condition that the eigenvalues of the diffusion matrix $D = (D_{ij})$ must be real and positive [4].

Positive cross-diffusion coefficients tend to separate the corresponding species, whereas negative ones drive their local accumulation, i.e., cross diffusion can generate spatial patterns [5]. Experiments on chemical systems show that the values of the cross-diffusion coefficients are often comparable to, or larger than, the main (diagonal) diffusion coefficients [6–9]. In light of this fact, it is significant that pattern formation can occur already for small values of the cross-diffusion constants if the kinetics are nonlinear [5]. The interplay of diffusion and kinetics described by the theory of the Turing instability has been recently discussed in this context and the conditions for the Turing instability were examined in the presence of cross diffusion with density-dependent coefficients of a general type [10]. We focus here on the description of the regions of parameter space where the conditions for pattern formation via the Turing instability are satisfied. For simplicity, we consider a linear concentration dependence of the cross-diffusion coefficients as in (1.1) and analyze the two basic classes of two-variable reaction-diffusion systems, namely cross activator-inhibitor systems and pure activator-inhibitor systems. A typical example belonging to the first class is the Brusselator model [11,12], one of the most frequently studied model systems in pattern formation, with reaction functions

$$F_1(u,v) = A - (B+1)u + u^2 v, \quad (1.2a)$$

$$F_2(u,v) = Bu - u^2 v, \quad (1.2b)$$

where A and B are positive constants. The dimensionless concentration of the activator is given by u and that of the inhibitor by v. A typical example belonging to the second class is the two-variable Oregonator model of the Belousov-Zhabotinsky reaction [13,14] with reaction functions

$$F_1(u,v) = \frac{1}{\epsilon}\left[u - u^2 - f v\frac{u-q}{u+q}\right], \quad (1.3a)$$

$$F_2(u,v) = u - v, \quad (1.3b)$$

where ϵ, f, and q are positive constants.

The paper is organized as follows. In Sec. II, we obtain the conditions for the Turing instability and indicate the regions of parameter space for which linear stability analysis predicts pattern formation. In Sec. III, the character of these regions is specified in more detail using the amplitude equation obtained by weakly nonlinear analysis. In Sec. IV, we discuss our results and highlight universal features of the Turing instability analysis that allow us to carry out a large reduction in the number of required parameters. We discuss the importance of including cross-diffusion terms in reaction-diffusion systems, mention open problems, and summarize our results in Sec. V. Technical details of the derivation of the amplitude equation are collected in the Appendix.

II. TURING INSTABILITY

A Turing bifurcation corresponds to a diffusion-driven instability of a homogeneous steady state that is stable to homogeneous perturbation, i.e., it is a stable steady state of the well stirred system corresponding to (1.1) without the diffusion terms, but is unstable within the full reaction-diffusion system. The conditions for the steady state to be stable against

*zemskov@ccas.ru
†klaus.kassner@ovgu.de
‡marcus.hauser@ovgu.de
§whorsthe@mail.smu.edu

homogeneous perturbations are that the Jacobian J of the two-variable system has a negative trace and a positive determinant,

$$\text{tr } J < 0, \quad \det J > 0. \tag{2.1}$$

Taking into account that all eigenvalues of the diffusion matrix must be positive for chemical systems, we obtain a set of inequalities from the requirement that the steady state be unstable against inhomogeneous perturbations. In general, Turing patterns are observed if the following four conditions are satisfied [10,15]:

$$\det \hat{D} = \hat{D}_{11}\hat{D}_{22} - \hat{D}_{12}\hat{D}_{21} > 0, \tag{2.2a}$$
$$(\hat{D}_{11} - \hat{D}_{22})^2 + 4\hat{D}_{12}\hat{D}_{21} \geqslant 0, \tag{2.2b}$$
$$\hat{D}_{11}J_{22} + \hat{D}_{22}J_{11} - \hat{D}_{12}J_{21} - \hat{D}_{21}J_{12} > 0, \tag{2.2c}$$
$$(\hat{D}_{11}J_{22} + \hat{D}_{22}J_{11} - \hat{D}_{12}J_{21} - \hat{D}_{21}J_{12})^2 - 4 \det \hat{D} \det J \geqslant 0, \tag{2.2d}$$

where the J_{ij} are the elements of the Jacobian and the $\hat{D}_{ij}$ are the elements of the effective diffusion matrix,

$$\hat{D} = \begin{pmatrix} D_{11} & D_{12}u_0 \\ D_{21}v_0 & D_{22} \end{pmatrix}. \tag{2.3}$$

Here (u_0, v_0) is the steady state of the spatially homogeneous system, given by $F_1(u_0, v_0) = F_2(u_0, v_0) = 0$.

The first two inequalities, (2.2a) and (2.2b), ensure the positivity of the eigenvalues of the effective diffusion matrix. [We consider only the case where the diagonal diffusion coefficients are positive. The thermodynamic requirement that $D_{11} + D_{22} > 0$ is automatically fulfilled and is not included explicitly in (2.2).] The last two inequalities are obtained from a stability analysis of the linearized reaction-diffusion system,

$$\frac{\partial X}{\partial t} = J_{11}X + J_{12}Y + \hat{D}_{11}\frac{\partial^2 X}{\partial r^2} + \hat{D}_{12}\frac{\partial^2 Y}{\partial r^2}, \tag{2.4a}$$
$$\frac{\partial Y}{\partial t} = J_{21}X + J_{22}Y + \hat{D}_{21}\frac{\partial^2 X}{\partial r^2} + \hat{D}_{22}\frac{\partial^2 Y}{\partial r^2}, \tag{2.4b}$$

for small perturbations X and Y of the steady state (u_0, v_0), namely $u = u_0 + X, v = v_0 + Y$. The inequality (2.2c) is a necessary, but not a sufficient, condition for a Turing instability. The Turing threshold corresponds to the case where the equal sign applies in the last inequality (2.2d). The inequalities (2.2) define a domain in parameter space, called the pattern formation space or Turing space [16].

A. Brusselator

The Brusselator model admits a steady state $u_0 = A$, $v_0 = B/A$, and the Jacobian at this steady state reads

$$J = \begin{pmatrix} B-1 & A^2 \\ -B & -A^2 \end{pmatrix}. \tag{2.5}$$

The Jacobian has the sign structure

$$J = \begin{pmatrix} + & + \\ - & - \end{pmatrix}, \tag{2.6}$$

if $B > 1$, which is the signature of a cross activator-inhibitor system. The determinant $\det J = A^2$ is always positive. The stability of the steady state in the well stirred system is therefore entirely determined by the condition on the trace; see (2.1). This restricts the values of the parameter B to $B < 1 + A^2 = B_c^H$, where B_c^H is the critical value for the Hopf bifurcation, which corresponds to the threshold of oscillations in the well stirred system.

The effective diffusion matrix of the linearized reaction-diffusion system is given by

$$\hat{D} = \begin{pmatrix} D_{11} & D_{12}A \\ D_{21}B/A & D_{22} \end{pmatrix}. \tag{2.7}$$

Substitution of J and $\hat{D}$ into (2.2) yields the following conditions for the determination of the Turing region in the Brusselator model,

$$D_{11}D_{22} - BD_{12}D_{21} > 0, \tag{2.8a}$$
$$(D_{11} - D_{22})^2 + 4BD_{12}D_{21} \geqslant 0, \tag{2.8b}$$
$$-A^2D_{11} + (B-1)D_{22} + AB(D_{12} - D_{21}) > 0, \tag{2.8c}$$
$$[-A^2D_{11} + (B-1)D_{22} + AB(D_{12} - D_{21})]^2 - 4A^2(D_{11}D_{22} - BD_{12}D_{21}) \geqslant 0. \tag{2.8d}$$

A two-dimensional slice of the Turing space, the D_{12}-D_{21} plane, is represented in Fig. 1 for fixed values of the parameters A and B and different values of the ratio of the diagonal diffusion constants, $\Theta = D_{22}/D_{11}$. The effect of reducing this ratio is mostly to shift downwards and to the right that part of the boundary of the Turing region defined by the limiting case of inequality (2.8d). Each of the curves in the figure corresponds to a boundary of one of the domains described by the inequalities. Inequality (2.8a), for example, describes a

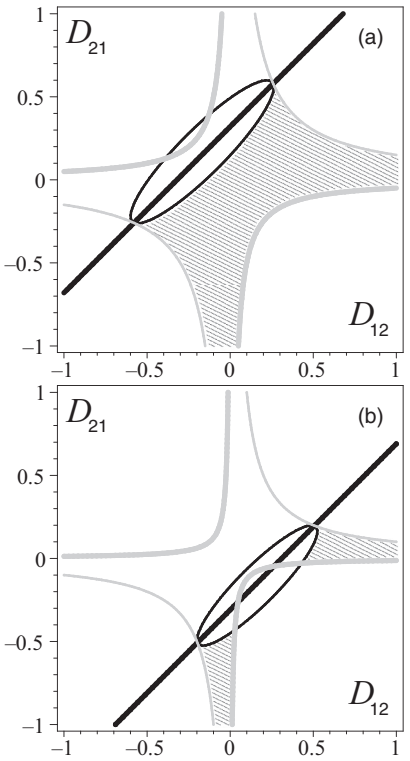

FIG. 1. Brusselator: pattern formation space for $A = 5$ and $B = 20$ with (a) $D_{11} = 1, D_{22} = 3$ and (b) $D_{11} = 2, D_{22} = 1$. Thin gray, thick gray, thick black, and thin black curves correspond to Eqs. (2.8a), (2.8b), (2.8c), and (2.8d), respectively. The Turing region corresponds to the hatched areas. All quantities are dimensionless.

region bounded by the product $D_{12}D_{21}$ taking on the positive value $D_{11}D_{22}/B$; thus the region is inside the two hyperbolas in the first and third quadrants. The second region is bounded by the product of D_{12} and D_{21} not becoming smaller than a certain negative value; the corresponding region is inside the hyperbolas lying in the second and fourth quadrants. The third inequality (2.8c) yields a straight line that divides the plane into two regions. Finally, the fourth inequality (2.8d) yields an elliptic region, outside of which the Turing region must lie.

We note that it is possible to enter the Turing region by crossing either of the three curves corresponding to the limiting cases of (2.2a), (2.2b), and (2.2d). The third inequality (2.2c) never determines the boundary of a region; it simply picks out into which of the two half planes the Turing region will fall. For the Brusselator, the Turing region lies below the straight line. The first two curves, corresponding to (2.2a) and (2.2b), provide the limits for the reaction-diffusion system to be an acceptable system in meeting the thermodynamic requirements on the diffusion matrix. The last curve, corresponding to (2.2d), then delimits the region of Turing instability within the domain of thermodynamically acceptable systems.

Figure 1 shows two different situations: (a) the case where *both* cross-diffusion coefficients can vanish simultaneously in the Turing region [Fig. 1(a), the origin is inside the hatched region], and (b) the case where *only one* cross-diffusion constant can take on the value zero inside the hatched region [Fig. 1(b)]. The first case includes the situation where the Turing instability occurs in systems without cross-diffusion terms and which requires that the main diffusion coefficient of the inhibitor is larger the main diffusion coefficient of the activator, $D_{22} > D_{11}$. In the second case, cross diffusion contributes crucially to the pattern formation and the inhibitor need not diffuse faster than the activator.

Using the inequality (2.8d), we obtain the critical value of the parameter B for the onset of the Turing instability in the Brusselator,

$$B_c = \frac{1}{\Delta_2^2}[\Delta_1\Delta_2 - 2\Delta_3 + \sqrt{(\Delta_1\Delta_2 - 2\Delta_3)^2 - (\Delta_2\Delta_4)^2}], \tag{2.9}$$

with notations $\Delta_1 \equiv A^2D_{11} + D_{22}$, $\Delta_2 \equiv D_{22} + A(D_{12} - D_{21})$, $\Delta_3 \equiv A^2D_{12}D_{21}$, and $\Delta_4 \equiv A^2D_{11} - D_{22}$. In the particular cases where $D_{21} = 0$ or $D_{12} = 0$, it reduces to

$$B_c = \frac{B_c^T}{1 + AD_{12}/D_{22}} \quad \text{or} \quad B_c = \frac{B_c^T}{1 - AD_{21}/D_{22}}, \tag{2.10}$$

respectively. Here $B_c^T = (1 + A\sqrt{D_{11}/D_{22}})^2$ is the critical value of B for the Turing instability in the Brusselator model without cross-diffusion terms. Since the parameter B must be positive, (2.10) implies the following restrictions on D_{12} and D_{21}: $D_{12} > -D_{22}/A$ and $D_{21} < D_{22}/A$ if the other cross-diffusion coefficient vanishes. In other words, the Turing instability will be suppressed if D_{12} becomes too negative or D_{21} becomes too positive. This fact was pointed out by Kumar and Horsthemke [10] for the Brusselator model with a general form of density-dependent cross-diffusion terms.

Writing the inhomogeneous spatial perturbations as $[X(r,t),Y(r,t)] = [X_0\exp(\lambda t + ikr), Y_0\exp(\lambda t + ikr)]$, we obtain the dispersion relation $\lambda(k)$ via linear stability analysis. The Turing instability corresponds to $\lambda(k_c) = 0$ with $k_c \neq 0$,

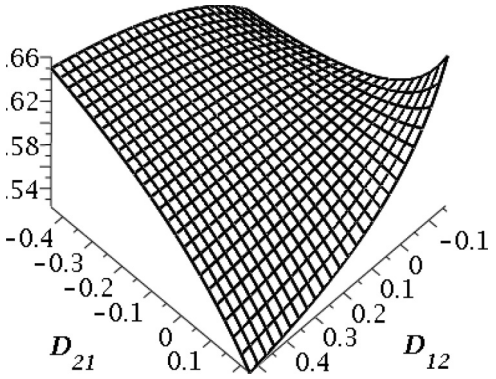

FIG. 2. Brusselator: length scale $1/k_c$ of the pattern formation for $A = 5$ and $D_{11} = 1, D_{22} = 3$, as in Fig. 1(a). All quantities are dimensionless.

and knowing B_c allows us to determine the critical wave number,

$$k_c^2 = \frac{A}{\sqrt{D_{11}D_{22} - B_cD_{12}D_{21}}}. \tag{2.11}$$

It provides a rough indication of the length scale to be expected in the emerging patterns. Figure 2 displays the dependence of this length scale $1/k_c$ on the cross-diffusion coefficients D_{12} and D_{21} for fixed diagonal diffusion coefficients. The behavior of the length scale changes from increasing to decreasing, or vice versa, when one cross-diffusion coefficient is varied and the other is fixed. The switch occurs when the line $D_{12} = 0$ or $D_{21} = 0$ is crossed. If D_{12} or D_{21} is equal to zero, then there is no cross-diffusion effect on k_c, as can be easily seen from (2.11) and which has also been shown in [10].

The Brusselator is a qualitative model of a cross activator-inhibitor chemical system, and all quantities are dimensionless. As far as real systems are concerned, Turing patterns have been observed experimentally in three different reaction-diffusion systems: (i) the chlorite-iodide-malonic acid reaction and its variant, the chlorine dioxide-iodine-malonic acid (CDIMA) reaction [17–19], (ii) the Belousov-Zhabotinsky reaction in a water-in-oil AOT (AOT is aerosol OT, and OT is the trademark for the surfactant sodium bis(2-ethylhexyl) sulfosuccinate) microemulsion (BZ-AOT reaction) [5,20], and (iii) reactions belonging to the class of pH oscillators [21,22]. The diffusion coefficients are on the order of 10^{-5} cm^2 s^{-1} for freely diffusing species in these reactions. They are one to two orders of magnitude smaller for those species that undergo complexation with a gel in the reactor in the case of reactions (i) and (iii) and for those species that are confined to the water droplets in the case of reaction (ii). Typical chemical time scales, set by the rate constants and the feed concentrations of the reactants, are on the order of one to ten minutes in the pattern-forming region of parameter space. The resulting wavelengths of the Turing patterns are about 0.2 mm for reactions (i) and (ii) and about 2 mm for reactions (iii).

B. Oregonator

The Oregonator model has a steady state,

$$u_0 = v_0 = \tfrac{1}{2}[1 - q - f + \sqrt{(1 - q - f)^2 + 4q(1 + f)}], \tag{2.12}$$

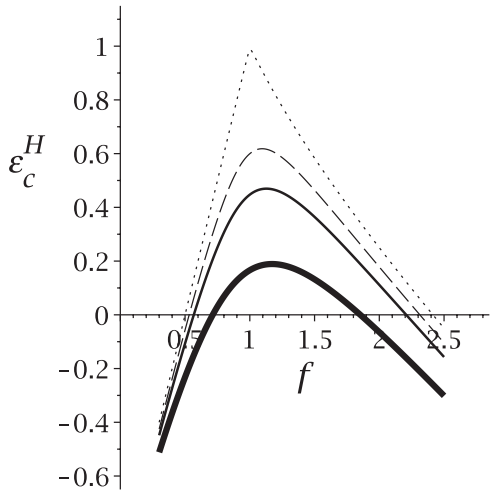

FIG. 3. Oregonator: boundary of the onset of the Hopf instability at the following values of q: 0.05 (thick), 0.02 (thin), 0.01 (dashed), and 10^{-5} (dotted line). All quantities are dimensionless.

and the elements of the Jacobian are

$$J_{11} = \varepsilon_c^H/\epsilon, \quad J_{12} = -\frac{f}{\epsilon}\frac{u_0 - q}{u_0 + q}, \\ J_{21} = 1, \quad J_{22} = -1. \tag{2.13}$$

Here

$$\varepsilon_c^H = 1 - 2u_0 - \frac{2qfu_0}{(u_0+q)^2}, \tag{2.14}$$

which is the critical value of the parameter ϵ for the onset of a Hopf instability. The Jacobian has the sign structure

$$J = \begin{pmatrix} + & - \\ + & - \end{pmatrix}, \tag{2.15}$$

which is the signature of a pure activator-inhibitor system. The stability of the steady state in the well stirred system, see (2.1), requires $\mathrm{tr}J < 0$. This restricts the values of ϵ to $\epsilon > \varepsilon_c^H$. Otherwise, the homogeneous steady state has already undergone a Hopf instability to homogeneous oscillations. Figure 3 shows the dependence of ε_c^H on the parameter f for different typical values of q. The requirement $\det J > 0$ produces the inequality

$$1 - 2u_0 - \frac{2qfu_0}{(u_0+q)^2} < f\frac{u_0 - q}{u_0 + q} \equiv \varepsilon^*, \tag{2.16}$$

which is satisfied for typical values of q and f.

Appropriate values q, f, and ϵ, chosen from Fig. 3, are used for the conditions to determine the Turing region in the Oregonator model,

$$D_{11}D_{22} - u_0^2 D_{12}D_{21} > 0, \tag{2.17a}$$

$$(D_{11} - D_{22})^2 + 4u_0^2 D_{12}D_{21} \geqslant 0, \tag{2.17b}$$

$$-D_{11} + \frac{\varepsilon_c^H}{\epsilon}D_{22} - u_0 D_{12} + \frac{\varepsilon^*}{\epsilon}u_0 D_{21} > 0, \tag{2.17c}$$

$$\left[-D_{11} + \frac{\varepsilon_c^H}{\epsilon}D_{22} - u_0 D_{12} + \frac{\varepsilon^*}{\epsilon}u_0 D_{21}\right]^2 \\ - \frac{4}{\epsilon}(D_{11}D_{22} - u_0^2 D_{12}D_{21})\left(\varepsilon^* - \varepsilon_c^H\right) \geqslant 0. \tag{2.17d}$$

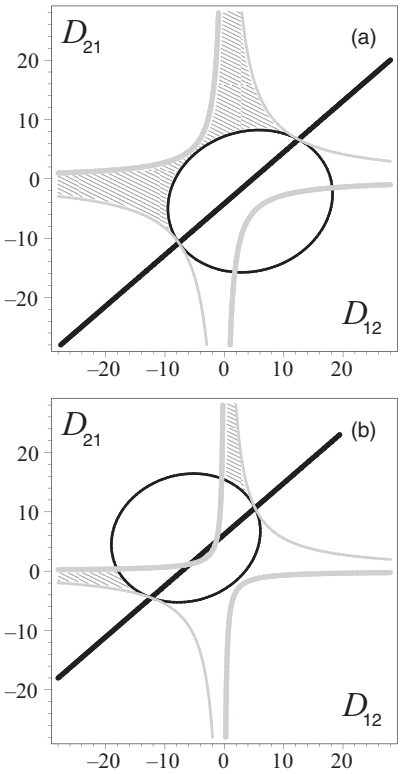

FIG. 4. Oregonator: pattern formation space for $q = 0.02$, $f = 1$, and $\epsilon = 0.7$ with (a) $D_{11} = 1, D_{22} = 3$ and (b) $D_{11} = 2, D_{22} = 1$. Thin gray, thick gray, thick black, and thin black curves correspond to Eqs. (2.17a), (2.17b), (2.17c), and (2.17d), respectively. The Turing region corresponds to the hatched areas. All quantities are dimensionless.

The Turing space for the Oregonator is shown in Fig. 4 for the same $\Theta = D_{22}/D_{11}$ values as in Fig. 1. For this model, the circumstances for pattern formation are most favorable if $D_{12} < 0$ and $D_{21} > 0$, as was mentioned by Chung and Peacock-López [15] for the templator model with cross-diffusion terms. The regions given by the general inequalities (2.2) are slightly modified compared to those for the Brusselator, and Turing patterns are allowed in the regions *above* the straight line, here given by (2.17c), instead of *below*, as in Fig. 1. For the Oregonator, a pure activator-inhibitor system, we have a kind of inverted situation compared to the Brusselator, a cross activator-inhibitor system. Except for this inversion, the Turing regions in the D_{12}-D_{21} plane for the two models are essentially similar, which allows us to restrict the discussion to the Brusselator model from now on.

III. TURING PATTERNS

In order to determine the long-time dynamical evolution, in particular to find a possible saturation amplitude of the Turing pattern and its overall character, nonlinear effects of (1.1) and (1.2) must be taken into account. Close to the threshold of the instability, these equations can be transformed into weakly nonlinear evolution equations for small perturbations X and Y of the steady state, i.e.,

$$\partial_t X = f_1(X,Y) + D_{11}\partial_r^2 X + D_{12}\partial_r[(A+X)\partial_r Y], \tag{3.1a}$$

$$\partial_t Y = f_2(X,Y) + D_{21}\partial_r[(B/A+Y)\partial_r X] + D_{22}\partial_r^2 Y, \tag{3.1b}$$

where the new reaction functions,

$$f_1(X,Y) = (B-1)X + A^2 Y + \frac{B}{A}X^2 + 2AXY + X^2 Y, \tag{3.2a}$$

$$f_2(X,Y) = -BX - A^2 Y - \frac{B}{A}X^2 - 2AXY - X^2 Y, \tag{3.2b}$$

are different from the original ones given in (1.2). If the set of equations (3.1) and (3.2) leads to solutions with a small saturating amplitude, then the weakly nonlinear expansion is justified *a posteriori*, sufficiently close to the threshold.

The form of the perturbations X and Y reflects the type of the emerging pattern. The simplest possibility is a modulation with a wave number close to the critical value k_c. In a one-dimensional setting and with $k_c \neq 0$, this is also the only possibility for a codimension one bifurcation. In two spatial dimensions, if we read the spatial derivatives in (3.1) as gradients, states comprising several nonaligned wave vectors and describing squares or hexagons can occur. A one-dimensional perturbation would be described as a stripe pattern in higher dimensions, but since we consider here a one-dimensional basic set of equations, we will just speak of Turing patterns.

In the vicinity of the Turing instability, these patterns can be described by amplitude equations derived through a weakly nonlinear analysis using the method of multiple scales. For the system (1.1) and (1.2), the amplitude equation

$$\frac{\partial W}{\partial t} = \eta W + g\,|W|^2 W + \mathcal{D}\frac{\partial^2 W}{\partial r^2}, \tag{3.3}$$

where the function $W = W(r,t)$ is the complex amplitude, has the following coefficients (for details of their derivation see the Appendix):

$$\eta = \frac{1}{1+\alpha\beta}\left[1-\beta\left(1+D_{21}k_c^2/A\right)\right](B-B_c), \tag{3.4}$$

$$\mathcal{D} = \frac{4k_c^2}{1+\alpha\beta}\frac{(D_{11}+\alpha A D_{12})(AD_{12}+\beta D_{22})}{A\left(A-D_{12}k_c^2\right)}, \tag{3.5}$$

$$\begin{aligned} g = \frac{1}{1+\alpha\beta}\big[&3\alpha(1-\beta) + 2(B_c/A)\hat{a}_2 \\ &+ 2(1-\beta)A(\hat{b}_0+\hat{b}_2+\alpha\hat{a}_2) + D_{12}k_c^2(\alpha\hat{a}_2 - 2\hat{b}_2) \\ &+ \beta D_{21}k_c^2(\hat{b}_2 - \hat{b}_0 - 2\alpha\hat{a}_2)\big], \end{aligned} \tag{3.6}$$

where

$$\alpha = -\frac{B_c - 1 - D_{11}k_c^2}{A^2 - D_{12}Ak_c^2} = -\frac{B_c + D_{21}(B_c/A)k_c^2}{A^2 + D_{22}k_c^2}, \tag{3.7}$$

$$\beta = \frac{A^2 - D_{12}Ak_c^2}{A^2 + D_{22}k_c^2} = \frac{B_c - 1 - D_{11}k_c^2}{B_c + D_{21}(B_c/A)k_c^2}, \tag{3.8}$$

and

$$\hat{b}_0 = -(2/A^3)(B_c + 2\alpha A^2), \tag{3.9a}$$

$$\hat{a}_2 = \frac{c_{22}c_{01} - c_{02}c_{12}}{c_{11}c_{22} - c_{12}c_{21}}, \tag{3.9b}$$

$$\hat{b}_2 = \frac{c_{11}c_{02} - c_{01}c_{21}}{c_{11}c_{22} - c_{12}c_{21}}, \tag{3.9c}$$

with

$$c_{11} = -B_c + 1 + 4D_{11}k_c^2, \tag{3.10a}$$

$$c_{12} = -A^2 + 4AD_{12}k_c^2, \tag{3.10b}$$

$$c_{21} = B_c + 4(B_c/A)D_{21}k_c^2, \tag{3.10c}$$

$$c_{22} = A^2 + 4D_{22}k_c^2, \tag{3.10d}$$

$$c_{01} = B_c/A + 2\alpha\left(A - D_{12}k_c^2\right), \tag{3.10e}$$

$$c_{02} = -B_c/A - 2\alpha\left(A + D_{21}k_c^2\right). \tag{3.10f}$$

The sign of g determines the nature of the Turing instability: the system undergoes a supercritical bifurcation if g is negative and a subcritical bifurcation if g is positive. In the first case, the cubic amplitude equation can be expected to provide a satisfactory description of the system dynamics sufficiently close to the instability threshold. In the latter case, the nonlinear analysis has to be extended at least to fifth order, and this may not be sufficient to accurately capture finite-amplitude effects then arising. Even if the fifth-order term leads to saturation, one cannot be sure that the fifth-order equation constitutes a good approximation, because there is no way of making the amplitude arbitrarily small. It jumps to a finite value at the instability threshold, and this value may be too large to allow truncation at the fifth order with sufficient accuracy. The only case where arbitrary accuracy can be attained with fifth-order amplitude equations, and not with cubic ones, is that of a tricritical point, i.e., if $g = 0$, because then the amplitude becomes arbitrarily small near the bifurcation point.

Figure 5 displays the regions with super- and subcritical bifurcations in the pattern formation space from Fig. 1(b).

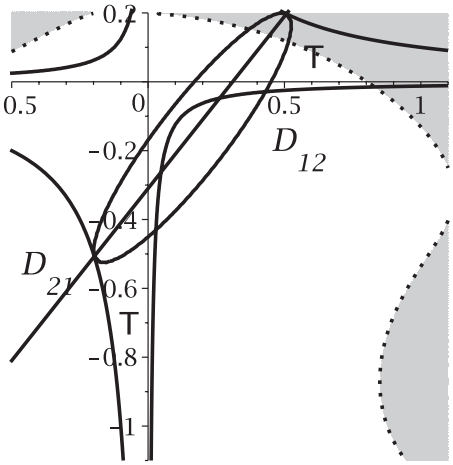

FIG. 5. Brusselator: pattern formation space with zones of subcritical (gray) and supercritical (white) bifurcation for $A = 5, B = 20$ and $D_{11} = 2, D_{22} = 1$, as in Fig. 1(b). Turing regions correspond to the area between the curves marked "T." All quantities are dimensionless.

As mentioned in Sec. II B, the conditions for a Turing instability (2.2) give rise to an inverted situation for the Oregonator, a pure activator-inhibitor system, compared to the Brusselator, a cross activator-inhibitor system. Since the Turing space of both models is however essentially similar, except for this inversion, we expect that the results of the weakly nonlinear analysis apply qualitatively also to the Oregonator.

IV. DISCUSSION

Examining the diagrams of the pattern formation space in Fig. 1, one notes that they are symmetric with respect to the second bisector of the axes, i.e., the line $D_{12} + D_{21} = 0$. The Turing regions cover mostly only two (narrow) domains of increasing D_{12} or decreasing D_{21}, as the distance from the instability threshold is increasing. Note also that this symmetry in the D_{12}-D_{21} plane is present only within the linear analysis. It does not occur in the nonlinear analysis, see Fig. 5, and there is indeed no reason for it to remain preserved.

The antisymmetric influence of D_{12} and D_{21} can be understood by examination of (2.2), (2.5), and (2.13), which shows that the signs of the Jacobian elements $\left(\begin{smallmatrix}+&+\\-&-\end{smallmatrix}\right)$ for the Brusselator and $\left(\begin{smallmatrix}+&-\\+&-\end{smallmatrix}\right)$ for the Oregonator are responsible for this behavior. These sign structures of the Jacobian correspond to cross and pure activator-inhibitor systems, respectively, as discussed above.

Comparison of the Turing regions in the diagrams for the different values of the model parameters leads to the idea that the influence of the variation of the cross-diffusion coefficients on the size and the shape of the Turing regions is similar for different types of systems with cross diffusion. Since the system of inequalities (2.2) depends only on a particular linear combination of $\hat{D}_{12}$ and $\hat{D}_{21}$ as well as the product $\hat{D}_{12}\hat{D}_{21}$, we can simplify these conditions via the introduction of two new variables,

$$\Phi = \frac{1}{\hat{D}_{11}\hat{D}_{22}}\hat{D}_{12}\hat{D}_{21} \tag{4.1}$$

and

$$\Psi = \xi^{-1}(\hat{D}_{11}J_{22} + \hat{D}_{22}J_{11} - \hat{D}_{12}J_{21} - \hat{D}_{21}J_{12}), \tag{4.2}$$

with $\xi = 2\sqrt{\hat{D}_{11}\hat{D}_{22}\det J}$. We obtain the three inequalities

$$-\chi \leqslant \Phi < 1, \quad \Psi > 0, \quad \Phi \geqslant 1 - \Psi^2, \tag{4.3}$$

where

$$\chi = \frac{1}{4}\left(\frac{\hat{D}_{11}}{\hat{D}_{22}} + \frac{\hat{D}_{22}}{\hat{D}_{11}} - 2\right) = \frac{1}{4d^2}(1-d^2)^2, \tag{4.4}$$

and the notation $d \equiv \sqrt{\hat{D}_{11}/\hat{D}_{22}}$ for the ratio of the effective diagonal diffusion coefficients has been introduced.

The inequalities (4.3) determine the Turing region in terms of a linear combination, Ψ, and the product, Φ, of the cross-diffusion coefficients and contain only one parameter, χ, which depends solely on the ratio of the diagonal diffusion constants. When they are equal, χ vanishes so that $\hat{D}_{12}$ and $\hat{D}_{21}$ have the same sign, or are equal to zero. In this case, the Turing region has a minimal size. The form (4.3) is universal, reducing an eight-parameter problem to a three-parameter one, into which the kinetics enter only via the single parameter Ψ. The generic shape of the Turing regions is thus fixed for a great variety of reaction-diffusion systems.

There is a limitation to the present consideration, which does not refer to the nonlinear behavior in any case. In our approach we consider only the regime of small and moderate concentrations for the activator and inhibitor. If the concentrations become too large, a linear density dependence of the cross-diffusion coefficients violates the thermodynamic conditions (2.2a) or (2.2b). At sufficiently large concentrations, the cross-diffusion coefficients must deviate from linear behavior. For example, they could display saturation effects, $D_{12}(u) = \tilde{D}_{12}u/(u + \delta_u)$, where $\delta_u \gg 1$, and a similar form for $D_{21}(v)$. Then for $u \ll \delta_u$, we obtain $D_{12}(u) = \tilde{D}_{12}u/\delta_u = D_{12}u$, i.e., the linear dependence used in (1.1), with $D_{12} = \tilde{D}_{12}/\delta_u$. A more detailed discussion of this question is outside the scope of this paper [23].

V. CONCLUSION

Cross-diffusion effects can play an important role in chemical reactions in the gas phase and fluid flows, at a surface, and in solution. An example for the first case is combustion, where cross diffusion acts on all variables. In hydrogen-air flames at atmospheric pressure, for instance, cross-diffusion effects are comparable to the main diffusion effects [24]. As expected, cross diffusion plays an important role in the dynamics of flame fronts [25,26]. Numerical studies show that neglecting cross-diffusive effects produces estimates of the flame front thickness that disagree with experimental data [26].

An example for the role of cross-diffusive effects in surface reactions is the $O_2 + H_2$ reaction on a Rh(110) surface doped with the promotor K [27,28]. The latter is a mobile species adsorbed on the Rh surface and enhances the rate of the catalytic reaction. This system is bistable and a reaction front propagates on the Rh surface. It leads to the formation of water and also redistributes the adsorbed potassium. The reaction front drags the potassium along and leads to its accumulation. When two reducing fronts, i.e., reaction fronts that invade regions on the surface that are rich in oxygen, collide, they annihilate and form islands of coadsorbed oxygen and potassium of macroscopic size. After the shutoff of the supply of gaseous reactants, diffusion processes reestablish a homogeneous distribution of K on the Rh surface [27,28]. A three-variable model, where cross diffusion is included only in the evolution of the potassium concentration [27,29], produces numerical results in good agreement with the experimental observations.

For chemical reactions in solution, cross diffusion occurs in strong electrolytes, micelles, and microemulsions [5]. It has been established conclusively that cross-diffusive effects play an important role in the BZ-AOT reaction. Experiments show that cross-diffusion coefficients in this system are either comparable to or larger than the main diffusion coefficients [8,9,30]. Cross-diffusion effects are therefore expected to play a role in the pattern-forming mechanisms of this system [5]. We are not aware of any theoretical studies of the BZ-AOT reaction

that have explicitly included cross-diffusion terms in modeling this reaction. Cross diffusion in the CDIMA reaction system does not appear to have been studied experimentally, though such effects are expected to be present due to electrostatic, excluded volume, and complexation effects [5]. The effects of cross diffusion on the Turing instability in the CDIMA reaction have been studied theoretically [10] using the two-variable Lengyel-Epstein model [31,32] for that reaction. As far as the pH oscillator reaction-diffusion systems are concerned, neither theoretical nor experimental studies of cross-diffusive effects exist to our knowledge.

We have investigated the effects of cross-diffusion terms, specifically terms that depend linearly on concentration, on the Turing space of two-variable reaction-diffusion systems. We have explicitly considered an example of a pure activator-inhibitor system as well as an example of a cross activator-inhibitor system. The Turing region is similar for both systems, modulo an inversion with respect to a straight line bisecting the D_{12}-D_{21} plane. Employing a weakly nonlinear analysis, we have derived an amplitude equation for the Turing patterns near the onset of instability, which allows us to determine whether the Turing bifurcation is supercritical or subcritical.

ACKNOWLEDGMENTS

E.P.Z. thanks Vladimir Vanag for the introduction into pattern formation, Anne De Wit for sending her Ph.D. thesis, and the German Academic Exchange Service (DAAD) for the Research Fellowship *Wiedereinladung 2012*.

APPENDIX: WEAKLY NONLINEAR ANALYSIS WITH MULTISCALE EXPANSION

In the vicinity of the instability, the control parameter $B \approx B_c$ and the concentrations u and v are expressed as expansions in the deviations X and Y from the steady state as [33]

$$\begin{pmatrix} u \\ v \end{pmatrix} = \begin{pmatrix} u_0 \\ v_0 \end{pmatrix} + \varepsilon \begin{pmatrix} X_1 \\ Y_1 \end{pmatrix} + \varepsilon^2 \begin{pmatrix} X_2 \\ Y_2 \end{pmatrix} + \varepsilon^3 \begin{pmatrix} X_3 \\ Y_3 \end{pmatrix} + \cdots , \tag{A1}$$

where the small expansion parameter ε is related to the distance μ from the instability via the expansion

$$\mu \propto B - B_c = \varepsilon B_1 + \varepsilon^2 B_2 + \cdots . \tag{A2}$$

Then the differential operators can be written as

$$\partial_t = \partial_{\tau_0} + \varepsilon \partial_{\tau_1} + \varepsilon^2 \partial_{\tau_2} + \cdots , \tag{A3a}$$

$$\partial_r = \partial_{\rho_0} + \varepsilon \partial_{\rho_1} + \varepsilon^2 \partial_{\rho_2} + \cdots . \tag{A3b}$$

Substituting (A1)–(A3) into (3.1) and (3.2) and collecting the terms at each order in ε, we obtain a set of equations,[1]

$$(\partial_{\tau_0} - L_c) \begin{pmatrix} X_n \\ Y_n \end{pmatrix} = \begin{pmatrix} I_{nx} \\ I_{ny} \end{pmatrix}, \quad n = 1,2,3, \ldots , \tag{A4}$$

where the matrix L_c,

$$L_c = \begin{pmatrix} B_c - 1 + D_{11}\,\partial^2_{\rho_0} & A^2 + D_{12} A\,\partial^2_{\rho_0} \\ -B_c + D_{21}(B_c/A)\,\partial^2_{\rho_0} & -A^2 + D_{22}\,\partial^2_{\rho_0} \end{pmatrix}, \tag{A5}$$

is calculated at the critical values of the control parameters.

[1] At the order ε^0, one recovers the steady state (u_0, v_0).

At the order ε^1 ($n = 1$), Eq. (A4) represents a linear equation with $I_{1x} = I_{1y} = 0$, whereas the equations at orders ε^2 and ε^3 are nonlinear and have the following right-hand sides:

$$\begin{pmatrix} I_{2x} \\ I_{2y} \end{pmatrix} = -\partial_{\tau_1} \begin{pmatrix} X_1 \\ Y_1 \end{pmatrix} + \left(\frac{B_c}{A} X_1^2 + 2 A X_1 Y_1 \right) \begin{pmatrix} 1 \\ -1 \end{pmatrix} + \begin{pmatrix} B_1 + 2 D_{11} \partial_{\rho_0} \partial_{\rho_1} & 2 D_{12} A \partial_{\rho_0} \partial_{\rho_1} \\ -B_1 + 2 D_{21} (B_c/A) \partial_{\rho_0} \partial_{\rho_1} & 2 D_{22} \partial_{\rho_0} \partial_{\rho_1} \end{pmatrix} \begin{pmatrix} X_1 \\ Y_1 \end{pmatrix}$$
$$+ \begin{pmatrix} 0 & D_{12} X_1 \partial^2_{\rho_0} + D_{12} \partial_{\rho_0} X_1 \partial_{\rho_0} \\ D_{21}(B_1/A + Y_1) \partial^2_{\rho_0} + D_{21} \partial_{\rho_0} Y_1 \partial_{\rho_0} & 0 \end{pmatrix} \begin{pmatrix} X_1 \\ Y_1 \end{pmatrix} \tag{A6}$$

and

$$\begin{pmatrix} I_{3x} \\ I_{3y} \end{pmatrix} = -\partial_{\tau_2} \begin{pmatrix} X_1 \\ Y_1 \end{pmatrix} + \left[\frac{2 B_c}{A} X_1 X_2 + 2 A (X_1 Y_2 + X_2 Y_1) + X_1^2 Y_1 \right] \begin{pmatrix} 1 \\ -1 \end{pmatrix}$$
$$+ \begin{pmatrix} B_2 + D_{11}\left(\partial^2_{\rho_1} + 2 \partial_{\rho_0} \partial_{\rho_2}\right) & D_{12} A \left(\partial^2_{\rho_1} + 2 \partial_{\rho_0} \partial_{\rho_2}\right) \\ -B_2 + D_{21}(B_c/A)\left(\partial^2_{\rho_1} + 2 \partial_{\rho_0} \partial_{\rho_2}\right) & D_{22}\left(\partial^2_{\rho_1} + 2 \partial_{\rho_0} \partial_{\rho_2}\right) \end{pmatrix} \begin{pmatrix} X_1 \\ Y_1 \end{pmatrix} + 2 \begin{pmatrix} D_{11} & D_{12} A \\ D_{21} B_c/A & D_{22} \end{pmatrix} \partial_{\rho_0} \partial_{\rho_1} \begin{pmatrix} X_2 \\ Y_2 \end{pmatrix}$$
$$+ \begin{pmatrix} D_{12}\left(X_2 \partial^2_{\rho_0} + 2 X_1 \partial_{\rho_0} \partial_{\rho_1} + \partial_{\rho_0} X_2 \partial_{\rho_0} + \partial_{\rho_0} X_1 \partial_{\rho_1} + \partial_{\rho_1} X_1 \partial_{\rho_0}\right) Y_1 + D_{12}\left(X_1 \partial^2_{\rho_0} + \partial_{\rho_0} X_1 \partial_{\rho_0}\right) Y_2 \\ D_{21}\left[(B_2/A + Y_2) \partial^2_{\rho_0} + 2 Y_1 \partial_{\rho_0} \partial_{\rho_1} + \partial_{\rho_0} Y_2 \partial_{\rho_0} + \partial_{\rho_1} Y_1 \partial_{\rho_0} + \partial_{\rho_0} Y_1 \partial_{\rho_1}\right] X_1 + D_{21}\left(Y_1 \partial^2_{\rho_0} + \partial_{\rho_0} Y_1 \partial_{\rho_0}\right) X_2 \end{pmatrix}, \tag{A7}$$

respectively.

The perturbations (X_1, Y_1) are proportional to the critical modes of L_c, the right eigenvectors of L_c with zero eigenvalue. In the case of the Turing instability, the right and left eigenvectors (column and row vectors) are

$$\begin{pmatrix} U_x \\ U_y \end{pmatrix} = \begin{pmatrix} 1 \\ \alpha \end{pmatrix} e^{i k_c \rho_0} \tag{A8}$$

and

$$(U_x^*, U_y^*) = \frac{1}{1+\alpha\beta}(1,\beta)e^{ik_c\rho_0}, \tag{A9}$$

respectively. Here α and β are given by (3.7) and (3.8).

The perturbations (X_1, Y_1) for the simplest one-dimensional (1D) pattern are built on one pair of opposite wave vectors [33],

$$\begin{pmatrix} X_1 \\ Y_1 \end{pmatrix} = \begin{pmatrix} 1 \\ \alpha \end{pmatrix} W e^{ik_c\rho_0} + \begin{pmatrix} 1 \\ \bar{\alpha} \end{pmatrix} \bar{W} e^{-ik_c\rho_0}, \tag{A10}$$

where $\bar{W}$ is the complex conjugate of the amplitude.

Substituting this expression into I_{2x} and I_{2y}, we write the solvability condition, the Fredholm alternative, $U_x^* I_{2x}^+ + U_y^* I_{2y}^+ = 0$ and $U_x^* I_{2x}^- + U_y^* I_{2y}^- = 0$, where I^+ and I^- are the coefficients of the terms proportional to $\exp(ik_c\rho_0)$ and $\exp(-ik_c\rho_0)$, respectively. For this solvability condition,

$$\begin{aligned} &-(1+\alpha\beta)\partial_{\tau_1} W + (1-\beta)B_1 W - \beta(B_1/A)D_{21}k_c^2 W \\ &+ 2ik_c[D_{11} + \alpha A D_{12} + \beta(B_c/A)D_{21} + \alpha\beta D_{22}]\partial_{\rho_1} W = 0, \end{aligned} \tag{A11}$$

we find

$$D_{11} + \alpha A D_{12} + \beta(B_c/A)D_{21} + \alpha\beta D_{22} = 0, \tag{A12}$$

and taking into account that $\partial_{\tau_1} W = \partial_{\tau_1} \bar{W} = 0$, we obtain $B_1 = 0$.

The deviations of second order are defined as [33]

$$\begin{pmatrix} X_2 \\ Y_2 \end{pmatrix} = \begin{pmatrix} a_0 \\ b_0 \end{pmatrix} + \begin{pmatrix} a_1 \\ b_1 \end{pmatrix} e^{ik_c\rho_0} + \begin{pmatrix} a_2 \\ b_2 \end{pmatrix} e^{2ik_c\rho_0} + \text{c.c.}, \tag{A13}$$

with c.c. as the notation for complex conjugate terms.

Substituting (X_1, Y_1) and (X_2, Y_2) into the second order of the multiscale expansion (A6) with $B_1 = 0$ and collecting the terms of the exponentials, we determine the coefficients a_n and b_n, with $n = 0, 1, 2$. They are given by

$$\begin{aligned} a_0 &= 0, \quad b_0 = \hat{b}_0 |W|^2, \\ a_2 &= \hat{a}_2 |W|^2, \quad b_2 = \hat{b}_2 |W|^2, \\ \alpha a_1 - b_1 &= 2ik_c \frac{D_{11} + \alpha A D_{12}}{A^2 - A D_{12} k_c^2} \partial_{\rho_1} W \\ &= -2ik_c \frac{\alpha D_{22} + (B_c/A)D_{21}}{A^2 + D_{22}k_c^2} \partial_{\rho_1} W, \end{aligned} \tag{A14}$$

with the quantities bearing a hat given in (3.9).

The cubic amplitude equation is obtained from the solvability condition $U_x^* I_{3x}^+ + U_y^* I_{3y}^+ = 0$ and $U_x^* I_{3x}^- + U_y^* I_{3y}^- = 0$, i.e.,

$$\begin{aligned} &-(1+\alpha\beta)\partial_{\tau_2} W + [1 - \beta(1 + D_{21}k_c^2/A)]B_2 W + 4k_c^2 \frac{(D_{11} + \alpha A D_{12})(A D_{12} + \beta D_{22})}{A\left(A - D_{12}k_c^2\right)} \partial_{\rho_1}^2 W + 2(B_c/A)\hat{a}_2 |W|^2 W + 2(1-\beta) \\ &\times A(\hat{b}_0 + \hat{b}_2 + \alpha\hat{a}_2)|W|^2 W + 3\alpha(1-\beta)|W|^2 W + D_{12}k_c^2(\alpha\hat{a}_2 - 2\hat{b}_2)|W|^2 W + \beta D_{21}k_c^2(\hat{b}_2 - \hat{b}_0 - 2\alpha\hat{a}_2)|W|^2 W = 0. \end{aligned} \tag{A15}$$

We multiply the equation by ε^3 and take into account that the amplitude W depends on the slow time and space variables τ_2 and ρ_1 only. Therefore, the leading-order terms on the right-hand side of (A3) disappear on application of the differential operators to W. Further, given that the distance from the instability threshold is of order ε^2, because $B_1 = 0$, we can make the formal replacements

$$\varepsilon^2 \partial_{\tau_2} = \partial_t, \quad \varepsilon \partial_{\rho_1} = \partial_r, \quad \varepsilon^2 B_2 = B - B_c, \tag{A16}$$

and $\varepsilon W \to W$. (Because the amplitude scales as the square root of the distance to the threshold, εW should be of order ε.) As a result of these steps, we obtain the amplitude equation in the final form (3.3) with coefficients (3.4)–(3.10).

[1] M. A. Tsyganov, J. Brindley, A. V. Holden, and V. N. Biktashev, Phys. Rev. Lett. **91**, 218102 (2003).
[2] E. F. Keller and L. A. Segel, J. Theor. Biol. **39**, 225 (1971).
[3] C. C. Lin and L. A. Segel, *Mathematics Applied to Deterministic Problems in the Natural Sciences* (SIAM, Philadelphia, 1988).
[4] D. G. Miller, V. Vitagliano, and R. Sartorio, J. Phys. Chem. **90**, 1509 (1986).
[5] V. K. Vanag and I. R. Epstein, Phys. Chem. Chem. Phys. **11**, 897 (2009).
[6] R. Mathew, L. Paduano, J. G. Albright, D. G. Miller, and J. A. Rard, J. Phys. Chem. **93**, 4370 (1989).
[7] O. Annunziata, L. Paduano, and J. G. Albright, J. Phys. Chem. B **110**, 16139 (2006).
[8] V. K. Vanag, F. Rossi, A. Cherkashin, and I. R. Epstein, J. Phys. Chem. B **112**, 9058 (2008).
[9] F. Rossi, V. K. Vanag, E. Tiezzi, and I. R. Epstein, J. Phys. Chem. B **114**, 8140 (2010).
[10] N. Kumar and W. Horsthemke, Phys. Rev. E **83**, 036105 (2011).
[11] R. Lefever, J. Chem. Phys. **49**, 4977 (1968).
[12] G. Nicolis and I. Prigogine, *Self-Organization in Nonequilibrium Systems* (Wiley, New York, 1977).
[13] J. J. Tyson and P. C. Fife, J. Chem. Phys. **73**, 2224 (1980).
[14] W. Jahnke, W. E. Skaggs, and A. T. Winfree, J. Phys. Chem. **93**, 740 (1989).
[15] J. M. Chung and E. Peacock-López, J. Chem. Phys. **127**, 174903 (2007); Phys. Lett. A **371**, 41 (2007).
[16] J. D. Murray, *Mathematical Biology* (Springer, Berlin, 2002).
[17] V. Castets, E. Dulos, J. Boissonade, and P. De Kepper, Phys. Rev. Lett. **64**, 2953 (1990).
[18] Q. Ouyang and H. L. Swinney, Nature (London) **352**, 610 (1991).
[19] Q. Ouyang and H. L. Swinney, Chaos **1**, 411 (1991).
[20] V. K. Vanag and I. R. Epstein, Phys. Rev. Lett. **87**, 228301 (2001).
[21] J. Horváth, I. Szalai, and P. De Kepper, Science **324**, 772 (2009).

[22] I. Szalai, J. Horváth, N. Takács, and P. De Kepper, Phys. Chem. Chem. Phys. **13**, 20228 (2011).
[23] V. Méndez, S. Fedotov, and W. Horsthemke, *Reaction-Transport Systems* (Springer, Berlin, 2010).
[24] B. Greenberg, Combust. Sci. Technol. **24**, 83 (1980).
[25] R. Hilbert, F. Tap, H. El-Rabii, and D. Thevenin, Prog. Energy Combust. Sci. **30**, 61 (2004).
[26] S. Palle, C. Nolan, and R. S. Miller, Phys. Fluids **17**, 103601 (2005).
[27] H. Marbach, M. Hinz, S. Günther, L. Gregoratti, M. Kiskinova, and R. Imbihl, Chem. Phys. Lett. **364**, 207 (2002).
[28] H. Marbach, G. Lilienkamp, H. Wei, S. Günther, Y. Suchorski, and R. Imbihl, Phys. Chem. Chem. Phys. **5**, 2730 (2003).
[29] M. Hinz, S. Günther, H. Marbach, and R. Imbihl, J. Phys. Chem. B **108**, 14620 (2004).
[30] F. Rossi, V. K. Vanag, and I. R. Epstein, Chem. Eur. J. **17**, 2138 (2011).
[31] I. Lengyel and I. R. Epstein, Science **251**, 650 (1991).
[32] I. Lengyel and I. R. Epstein, Proc. Natl. Acad. Sci. USA **89**, 3977 (1992).
[33] A. De Wit, Ph.D. thesis, Université Libre de Bruxelles, Brussels, 1993.